Geological 3D modelling for excavation activity in an underground marble quarry in the Apuan Alps (Italy)

Claudio Vanneschi [a*], Riccardo Salvini [a], Giovanni Massa [a], Silvia Riccucci [a], Angelo Borsani [a]

[a] University of Siena, Department of Environment, Earth and Physical Sciences and Centre for GeoTechnologies CGT. Via Vetri Vecchi 34, 52027, San Giovanni Valdarno (AR) Italy.

*Corresponding author. University of Siena, Department of Environment, Earth and Physical Sciences and Centre for GeoTechnologies CGT. Via Vetri Vecchi 34, 52027, San Giovanni Valdarno (AR) Italy. Tel.: +39 055 9119432. E-mail address: claudio.vanneschi@unisi.it (C. Vanneschi)

Abstract

The three-dimensional laser scanning technique has recently become common in diverse working environments. Even in geology, where further development is needed, this technique is increasingly useful in tackling various problems such as stability investigations or geological and geotechnical monitoring. Three-dimensional laser scanning supplies detailed and complete geometrical information in short working times, as a result of the acquisition of a large number of data-points that accurately model the detected surfaces. Moreover, it is possible to combine these data with high quality photographic images so as to provide important information for geological applications, as follows. A working approach, that combines terrestrial laser scanning and traditional geological surveys, is presented. A three-dimensional model, that includes information about the geological structure in an underground quarry in the Apuan Alps, is realized. This procedure is adaptable to other geological contexts, and because of its operating speed and accuracy it is invaluable for optimal excavation, in which a proper planning of quarrying activity is vital for safety and commercial reasons.

Key words: Underground quarrying; Apuan Alps; Terrestrial Laser Scanning; NURBS; 3D Modelling.

1. Introduction

In the planning of quarrying activity it is important to have accurate knowledge of the geometry of the study area, as well as its geological setting. As underground quarrying proceeds, it becomes harder to determine the absolute and relative position of distinct tunnels. This can give rise to problems, including from the security aspect. A combination of topographic, geological and engineering-geological information facilitates excavation plans that take into account stability conditions, and permits accurate prediction of the spatial location of marble varieties. In this context the Terrestrial Laser Scanning (TLS) provides significant advantages. TLS can be used to obtain detailed and complete geometrical information rapidly and accurately by generating clouds of points. Laser scanners with differing modality of data acquisition ("time-of-flight" and phase-based measurement) provide different degrees of precision and maximum measurable distances. In the present work a "time-of-flight" laser scanner was used. This instrument emits laser impulses along precise directions, and when these impulses reach a surface they are reflected back along their path (Petrie and Toth, 2008). The scanner analyzes the resulting information in order to determine the distance (ρ) of the points by time-of-flight (Δt) analysis:

$$\rho = c\Delta t / 2$$

where c = speed of light.

The position of each point is also determined in a spherical polar coordinate system by measurement of the azimuth and zenith angles. In this way every point has specific coordinates in a local reference system. At a later stage, by measuring optical targets positioned within the scanning area with a Total Station (TS) and GPS receivers, it is possible to georeference the clouds of points in an absolute reference system.

Attributes of TLS such as reliability, accuracy, safety and rapidity for geological applications have been repeatedly proven by several authors (Abellan et al. 2009; Armesto et al., 2009; Fekete et al. 2010; Lato et al. 2009; Salvini at al. 2013; Sturzenegger and Stead, 2009). Furthermore, TLS is not dependent on the lighting conditions and is therefore well suited to underground surveying. The rapidity of TLS does not affect the quality of the data, that generally has sub-centimetric accuracy (Boehler et al. 2003; Lemy et al. 2006; Lichti and Licht, 2006; Mechelke et al. 2007; Voegtle et al. 2008) and, consequently, a detailed and accurate topography of the excavation area can be generated. Another important aspect of TLS is that by overlaying high quality photographic data on to the point cloud, it is possible to generate a complete 3D view of the study area that is invaluable for geological interpretation and analysis. A detailed 3D view of the quarry is useful for both geological and engineering-geological surveys and, at a later stage, for validation of the newly produced geological maps and cross sections. This paper shows an example of working approach that involves the use of TLS, specific software, and geological and engineering-geological surveys in order to develop a three-dimensional model of an underground marble quarry. The advantages of this approach are discussed together with the reasons for the choices adopted in realizing an accurate, detailed and prompt solution.

2. Regional Geological Setting

The quarry under study, known as "Romana", is located in the Apuan Alps, in the Province of Massa-Carrara (Italy). The Apuan Alps metamorphic complex, composed of two major units, the Massa unit and the Apuan unit (Fig. 1), represents the largest tectonic window in the inner Northern Apennines where deep levels of the belt are exposed (Carmignani and Kligfield, 1990; Elter, 1975; Molli, 2008).

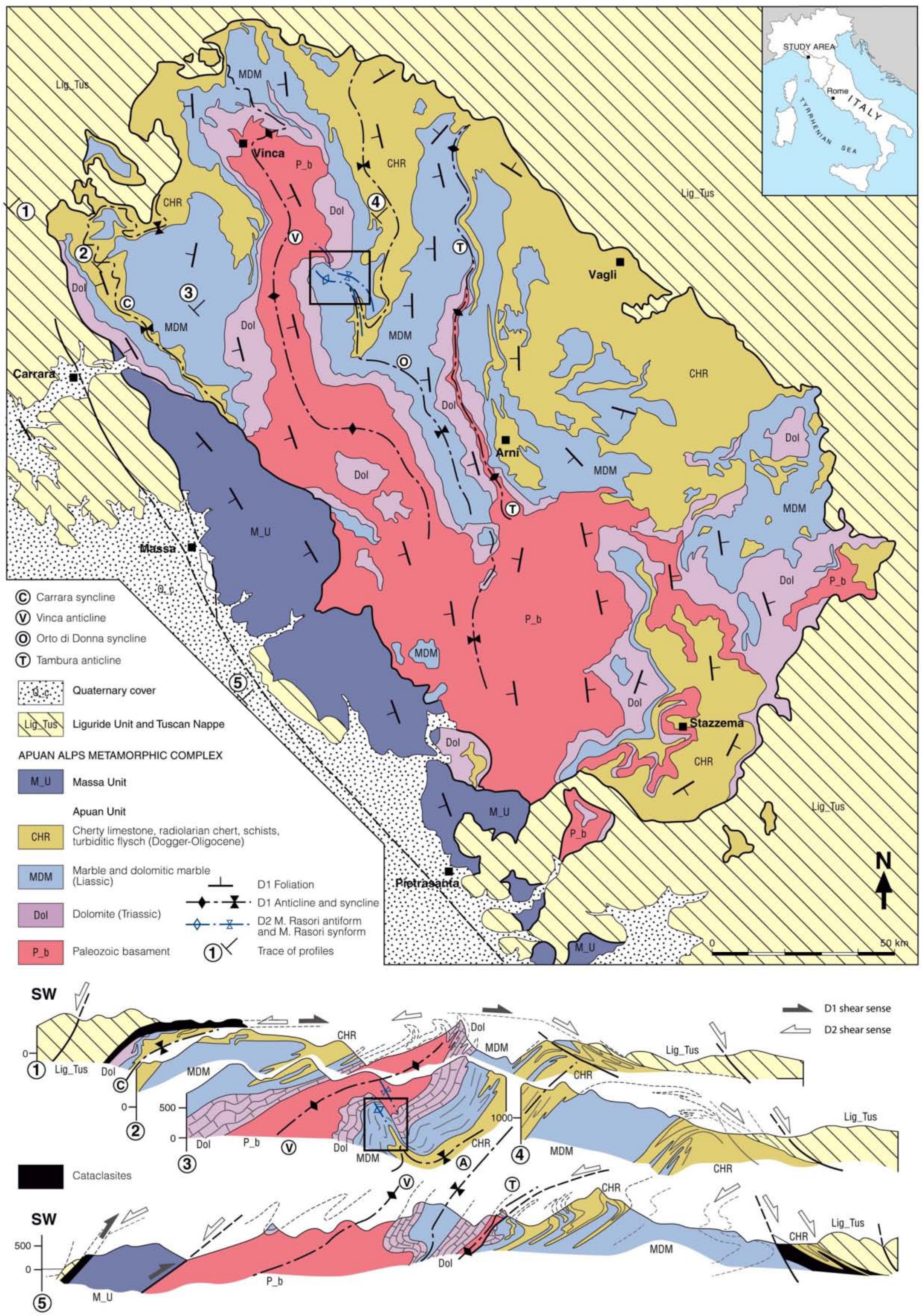

Fig. 1 - Geological sketch map of the Apuan Alps. The location of the quarry is highlighted with a black rectangle (modified after Conti et al., 2004)

The litho-stratigraphic sequence comprises a Paleozoic basement overlain unconformably by an Upper Triassic-Oligocene meta-sedimentary sequence. The Mesozoic cover rocks consist of thin Triassic continental to shallow water Verrucano-like deposits, followed by Upper Triassic-Liassic carbonate platform meta-sediments that include dolomites (“Grezzoni”), dolomitic marbles and marbles (worldwide known as “Carrara marbles”). These are overlain by Upper Liassic-Lower Cretaceous cherty meta-limestone, cherts and calcschists, and by lower Cretaceous-Lower Oligocene sericitic phyllites and calcschists, with marble interlayers, which are related to deep-water sedimentation during drowning of the former carbonate platform. Oligocene sedimentation of turbiditic sandstones (“Pseudomacigno”) completes the sedimentary history of the domain (Molli and Vaselli, 2006).

The regional tectonic setting of the Apuan Alps is the result of two main tectono-metamorphic events (D1 and D2 phases - Carmignani and Kligfield, 1990) which are regarded as recording progressive deformation of the distal Adriatic continental margin during continental subduction and the syn- to post-contractional exhumation (Molli and Meccheri, 2000; Molli et al., 2002; Molli and Meccheri, 2012). The ductile compressional event D1 was due to the Tertiary continental collision between the Sardinia-Corsica block and the Adria plate, and was followed by the D2 extensional event that led to a isostatic rebalance (Carmignani and Kligfield, 1990). During the D1 event, stacking took place of the tectonics unit belonging to the Tuscan and Ligurian domains, with development of a progressive deformation in two stages (Molli and Meccheri, 2000), the main of these represented by greenschist foliation (Sp) which is axial plane of isoclinal micro- to kilometric-scale folds.

This foliation, which characterizes most of the metamorphic rocks of the Apuan Alps, is associated with a stretching lineation SW-NE trending, interpreted as the main transport direction of the inner Northern Appennines (Carmignani et al., 1978; Molli, 2008). During the D2 event, the previously formed structures were reworked and developed different generations of folds and locally high strain zones associated with exhumation and vertical shearing (Molli, 2012). The result of this second deformative phase is a complex mega-antiform with Appenninic trending axis (NW-SE) (Carmignani and Kligfield, 1990). This trend is associated with non-cylindrical parasitic folds with sub-horizontal axial planar crenulations that involve transportation to the east on the eastern and to the west on the western limbs of the antiform (Carmignani & Kligfield, 1990; Carmignani et al., 1993a). Late stages of D2 are characterized by the development of brittle structures (low-angle, high-angle faults and joint systems) associated with the final exhumation and uplift of the metamorphic units in a frame of late to post-orogenic regional extension of the inner part of the Northern Apennine (Molli et al., 2010; Ottria and Molli, 2000). According to Fellin et al. (2007), Molli and Vaselli (2006), Molli et al. (2000, 2002) and references therein, the peak of metamorphism occurred in the early Miocene (at approximately 27 Ma; Kligfield et al., 1986), during the early D1 phase, at temperatures around 450-350 °C and pressure approximately 0.6 GPa. During the early stage of the D2 phase the metamorphism took place at a temperature above 250 °C. The structures associated with this last phase were dated at between 11 and 8 Ma according to zircon fission-track ages (Fellin et al., 2007).

3 Operational Framework

3.1 Geological surveying

To study the geological setting of the area, a new geological survey was carried out inside the quarry and surrounding area. All visible structural features, such as bedding, foliation, stretching lineations and fold axis were measured. A new geological map (Fig. 2) and four geological cross sections (Fig. 3), with structural elements projected along the medium D2 axis (348/25), were realized. This data has then been combined with a detailed engineering-geological survey carried out at a large scale with the help of geomatics as described later in the text.

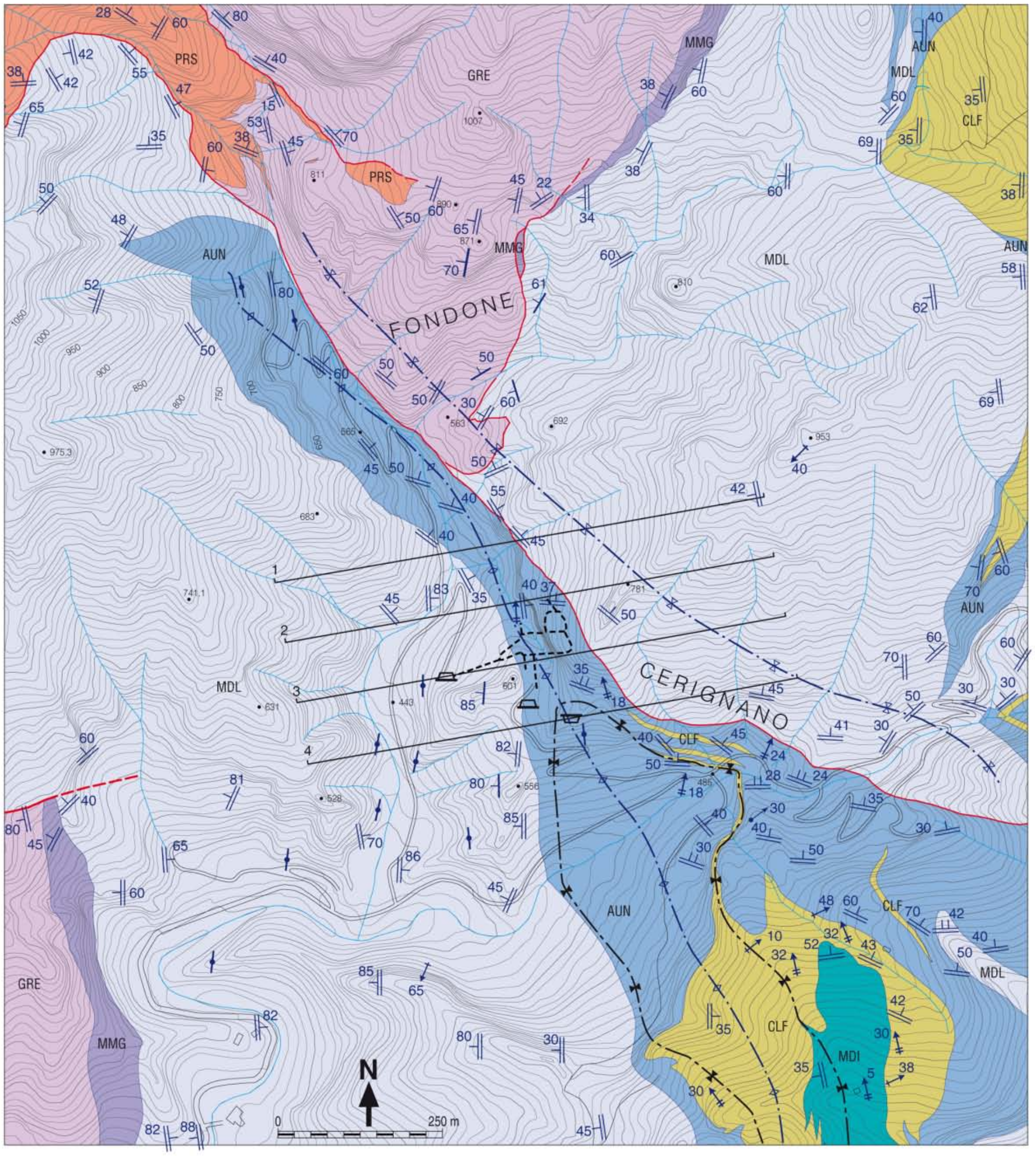

APUAN UNIT
Mesozoic and Tertiary succession

MDI — **METARADIOLARITES**
Red and green metaradiolarites, well bedded, with metapelites.
CALLOVIAN - TITONIAN

CLF — **CHERTY LIMESTONES**
Metacalcilutites with cherty layers and lenses, calcarenites, calcschists.
PLIENSBACHIAN p.p.

AUN — **MARBLE**
White and grey marble, marble breccias with interbedded dolomitic marbles. In the upper part well-layered white and gray-greenish marble.
HETTANGIAN

MDL — **DOLOMITIC MARBLES**
Alternating dolomitic marbles, dolomites and marbles.
HETTANGIAN

MMG — **MEGALODONT-BEARING MARBLES/SERAVEZZA BRECCIA**
Massive marbles with molluscs, brachiopods and megalodonts. Metamorphic polygenic breccias with marble and subordinate dolomite clasts, reddish and green phyllites, locally chloritoid-rich.
HETTANGIAN

GRE — **GREZZONI Fm.**
Dolomites in dm- to m-thick layers, of gray-black colour. Locally dolomitic breccias and dolomitic marbles.
NORIAN

Paleozoic Basement

PRS — **PORFIROIDI E SCISTI PORFIRICI Fm.**
Metavolcanic rocks, metarkoses, quartzites, phyllites.
MIDDLE ORDOVICIAN

- Geological boundary
- Tectonic contact
- Fault
- Orto di Donna syncline
- M. Rasori antiform
- M. Rasori synform
- 10 Inclined strata
- 15 Inclined main foliation (Sp)
- 15 Inclined S2 foliation
- Vertical main foliation (Sp_V)
- 60 D1 stretching lineation, mineral lineation (Lp)
- 60 Axis of D1 fold (Ap)
- 60 Axis of D2 fold (A2)
- Active quarry; inactive quarry
- Path of the tunnel
- A A' Cross section

Fig. 2 – Geological map of the Romana quarry and surrounding area

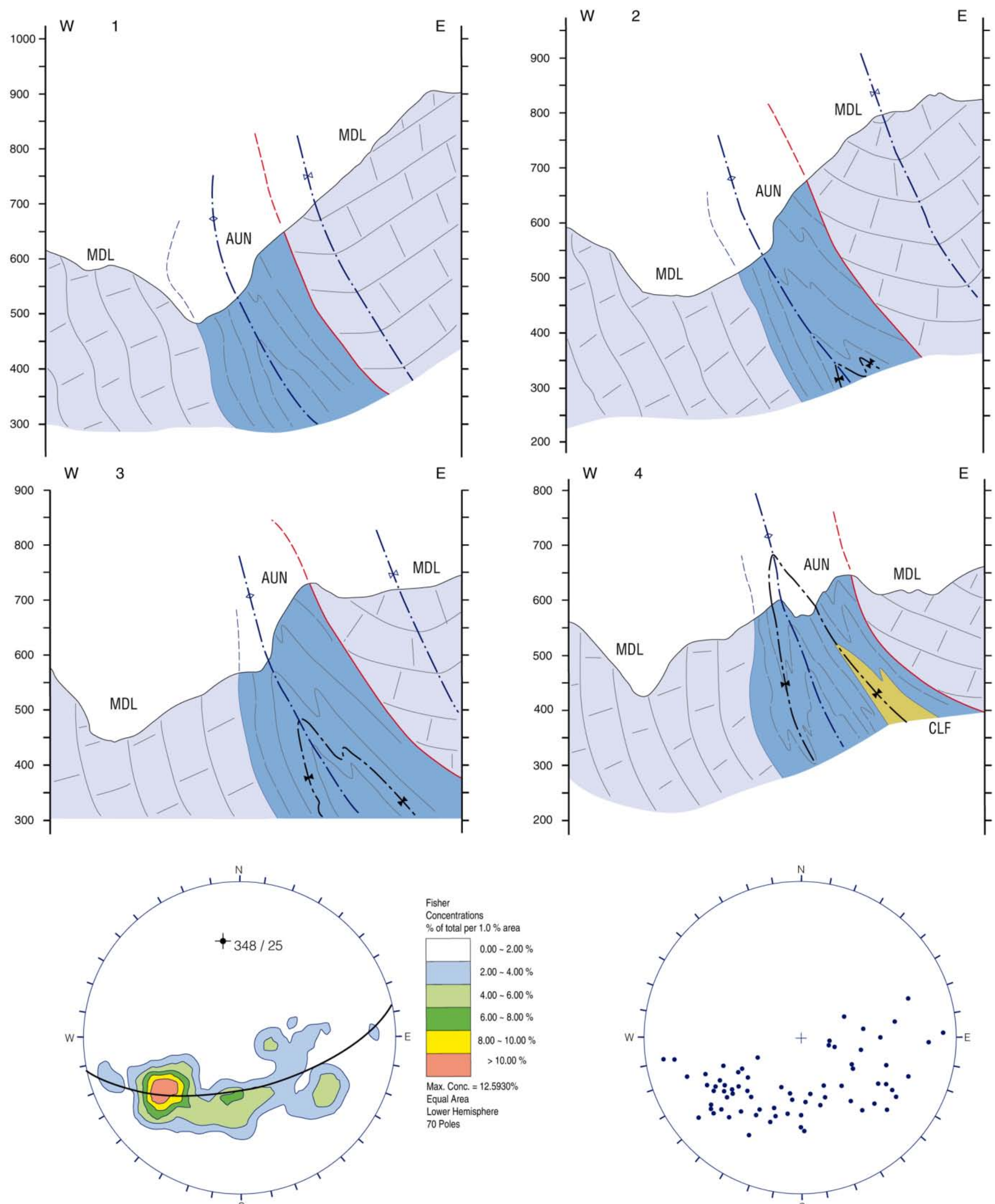

Fig. 3 – Geological cross sections of the Romana quarry and surrounding area (top); stereographic projection of Sp foliation measurements (n=70) through the lower-hemisphere of the Schmidt equal-area method (bottom).

The excavation activity of the quarry has proceeded underground within a late geological structure (D2) composed of Marble and Dolomitic Marble formations, known as the "Monte Rasori" antiform (Carmignani et al., 1993b). It is a fold structure located on the inverted limb of the "Orto di Donna" syncline belonging to the D1 phase. The syncline represents a first order E-NE vergent fold located on the central area of the Apuan Alps, with an amplitude of about 8 Km and a general N-S strike. The core of the structure is composed of Cherty Limestones and Metaradiolarites formations. The minor fold structures related to the D1 phase are isoclinals, mainly non-cylindrical and frequently recognizable as sheath folds. Their axial direction runs from NE to SW and is sub-parallel to the stretching lineation which, in the entire Apuan complex, shows a N60-80 trend. In association with these folds there is a pervasive axial-plane metamorphic foliation, which is high dipping and characterized by a dip direction toward E-NE.

In the study area the "Monte Rasori" antiform is associated with sub-vertical D1 foliations (Figg. 1, 2, and 3). Indeed, the "Orto di Donna" syncline in this area has been refolded leading to an unusual high angle D2 marble structure interpreted by Carmignani et al. (1993b) as a fold developed in shear zones confined by less competent rocks according to the model proposed by Rykkelid and Fossen (1992).

The marketable marble varieties extractable from the Romana quarry belong to the groups of *white marble* and *veined marble* (Carmignani et al., 2007). *Veined marble* is a meta-limestone that is variable in colour from pearl-white to very light gray, containing some often dense dark gray veins due to the presence of pyrite. Within this variety, metric or multimetric bands of middle to fine grain size marbles can be found, light gray coloured with dark gray to white veins. The most valuable variety from this quarry is known as "*Bianco P*", located in a narrow level having maximum thickness of about 3 m within the *white marble*. It is a white marble characterized by a middle/fine size grain (about 100 µm).

3.2 Terrestrial Laser Scanning

3.2.1 Point cloud acquisition

For TLS of the study area a *Leica*^{TM} *ScanStation2* was used (Fig. 4A). At 50 m from the origin, the instrument has an accuracy of 4 mm in distance and 6 mm in position; the spot size is 4 mm and the maximum scan density is less than 1 mm throughout the entire range. These specifications are suitable for geological applications of the present kind. This spot size, as noted by Lichti and Jamtsho (2006), is appropriate in geological environments where irregular surfaces frequently occur. The density chosen for scanning the Romana quarry was 6 cm at a distance of 50 m. In an underground quarry, however, the quarry walls are usually a few meters distant from the laser scanner origin, so that the density of points is almost everywhere greater. Moreover, the quality of the data acquired is high due to the characteristics of the material involved; as explained by Voegtle et al. (2008), the greatest accuracy and intensity of the reflected impulses are observed for smooth and light surfaces, similar to those encountered in the present study.

To survey the entire area, which is characterized by an elaborate network of tunnels having a total length of about 600 m, a total of 13 scans was conducted (managed with *Leica*^{TM} *Cyclone 8.0* software). The number of scans was chosen as a balance between minimizing possible occlusions and shadows in the output and amount of data that have to be acquired and processed. The output of every scan was a point cloud in which every point was defined by cartesian (x,y,z) coordinates relative to the scanner location and orientation. Each point cloud derives from the record of the "time-of-flight" and the intensity of the laser signal (Fig. 4B). To obtain a unique 3D model of the quarry a process of registration of all the point clouds is needed. To this end, by means of a topographic survey, the cartesian coordinates in an absolute reference system were acquired of some optical targets (Fig. 4C) located in particular positions within the excavation area. Locations were chosen so as to have a minimum of 5 visible targets in each single scan (to limit errors) and, if possible, few targets entering more than one scan. The advantage of this approach is that there is no multiplication effect of the error from the initial scan; the accuracy of the georeferencing process depends on topographic survey (Pejić, 2013). Moreover, the quarry has an irregular underground development but the entry and exit galleries correspond, and this shape makes it possible to adjust the error between the first and the last scans; the generation of a "closed polygonal outline" was used to reduce the error.

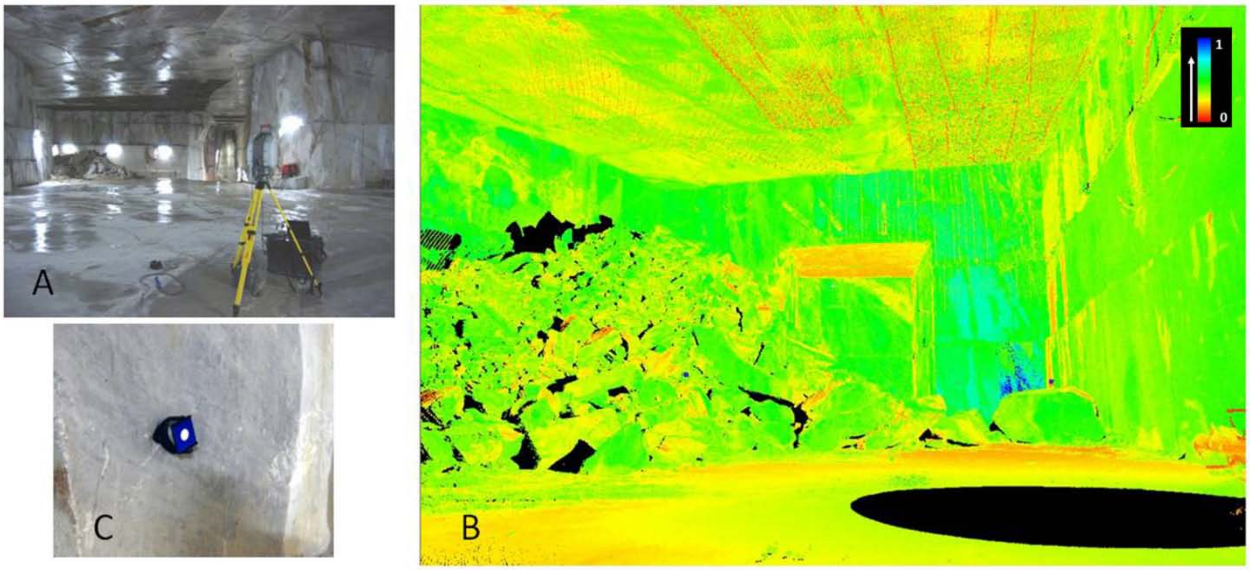

Fig. 4 –Leica^{TM} ScanStation2 during data acquisition (A); Point cloud represented by intensity values (B); detail of an optical target (C).

3.2.2 Topographic surveying

The topographic survey was carried out using a *Leica^{TM} TCRM 1205+R1000* Total Station (TS) and two *Leica^{TM}Viva* dual-frequency GPS receivers. The TS was used to measure the relative coordinates of selected points while GPS was used to determine the absolute coordinates of the origin of the survey and its reference direction (0-Azimuth direction).

TS instruments, which provide millimetric accuracy (Bertacchini et al., 2009; Beshr and Elnaga, 2011; Hill and Sippel, 2002; Kirschner & Stempfhuber, 2008; Kontogianni et al., 2007), are used increasingly in other fields of civil engineering, such as quarry surveying (Ganić et al., 2011; Lizzadro et al., 2007).

The two geodetic GPS receivers were set up on tripods and operated in static modality, receiving continuous signals from the satellites for a minimum of 3 hours. In this way, the coordinates of the two points were acquired both in the geographic (WGS84) and cartesian system (UTM-WGS84, Zone 32N).

The TS was then installed on the point chosen as the origin of the survey by replacing the GPS receiver; this point, with relative coordinates (0,0,0), was named “Base”. By using the second point of absolute coordinates as reference direction (0-Azimuth direction), the TS was initialized and targets visible on the first scan were measured. The further targets necessary to register all of the scans were acquired via the Intersection Method (IM) by moving the TS to different positions. With this method the new positions of the TS were resolved using a minimum of three points of known coordinates (previously measured targets). The IM error using this approach was always less than 5 mm. By using this technique more than 60 targets, with coordinates in the local reference system (origin at “Base”), were acquired. They were subsequently used, after the GPS post-processing, for the point clouds registration process that georeferenced the point clouds in an absolute reference system.

3.2.3 Acquisition of high resolution photos

After each scan, high resolution images were taken, replacing the TLS with a Nodal Ninja 3II series panoramic tripod head equipped with a Digital Nikon™ D80 camera. To obtain images of the entire surrounding area and generate a 360° panorama view, 42 pictures were needed. For three different vertical angles (-12°, 25° and 62°), one picture was acquired every 25.7° on the horizontal plane. The camera was set with a focal length of 18 mm, automatic focusing, and a diaphragm aperture of *f/8*, giving suitable depth of field and sharp images. The lighting conditions were variable in the study area (underground quarry with artificial lights), and the exposure time was determined case by case according to operator expertise.

4. TLS data processing

4.1 Processing of topographic data

GPS data were processed using *Leica™ Geo Office* software and differential methods by combining simultaneous records from three permanent GPS stations (*Borgo a Mozzano*, *La Spezia* and *Pieve*

Fosciana) and measuring the relative baselines (Fig. 5); permanent stations data were available on *Leica SmartNet ItalPos* official site (http://it.smartnet-eu.com/rinex-30-sec_568.htm). The orthometric height of the measured GPS points was calculated in collaboration with the Italian Military Geographic Institute. The processing facilitated adjustment of the measurements so as to achieve centimetric accuracy. By using the absolute coordinates of the two GPS points ("Base" and the point used for setting the TS 0-Azimuth direction), a 3D roto-translation of all the targets was performed. This made it possible to assign UTM-WGS84 Zone 32N coordinates (with orthometric height) to all the targets.

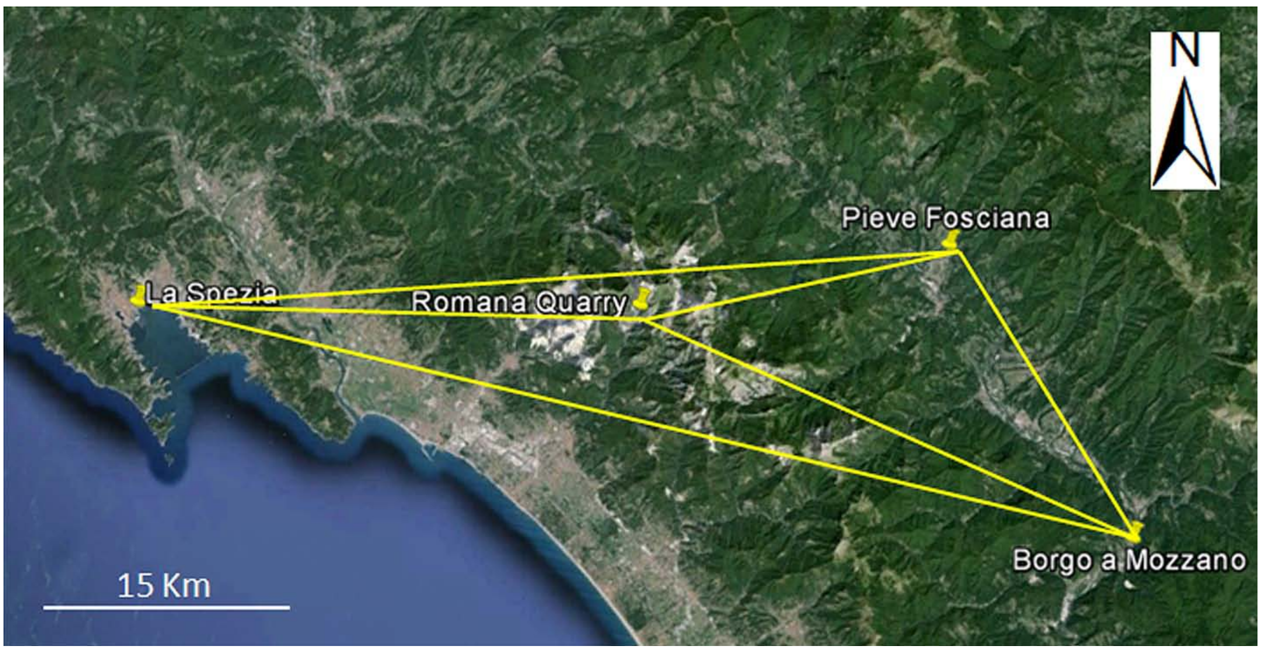

Fig. 5 - Location of permanent GPS stations with calculated baselines (modified from Google Earth™ 2013).

4.2 Processing of point clouds

The processed topographic data for all the targets allowed for georeferencing the point clouds using *Leica*^{TM} *Cyclone 8.0* software. This processing, called *registration*, makes it possible to refer all the point clouds to an unique reference system by applying a spatial transformation (3D roto-translation), using the targets as system constraints (Fig. 6). The accuracy achieved for the plano-altimetric alignment was sub-centimetric. Subsequently, with the aim of deleting all the irrelevant points acquired during the scans (e.g. trellis, cables, machines, instruments) a cleaning-up of the point clouds was undertaken.

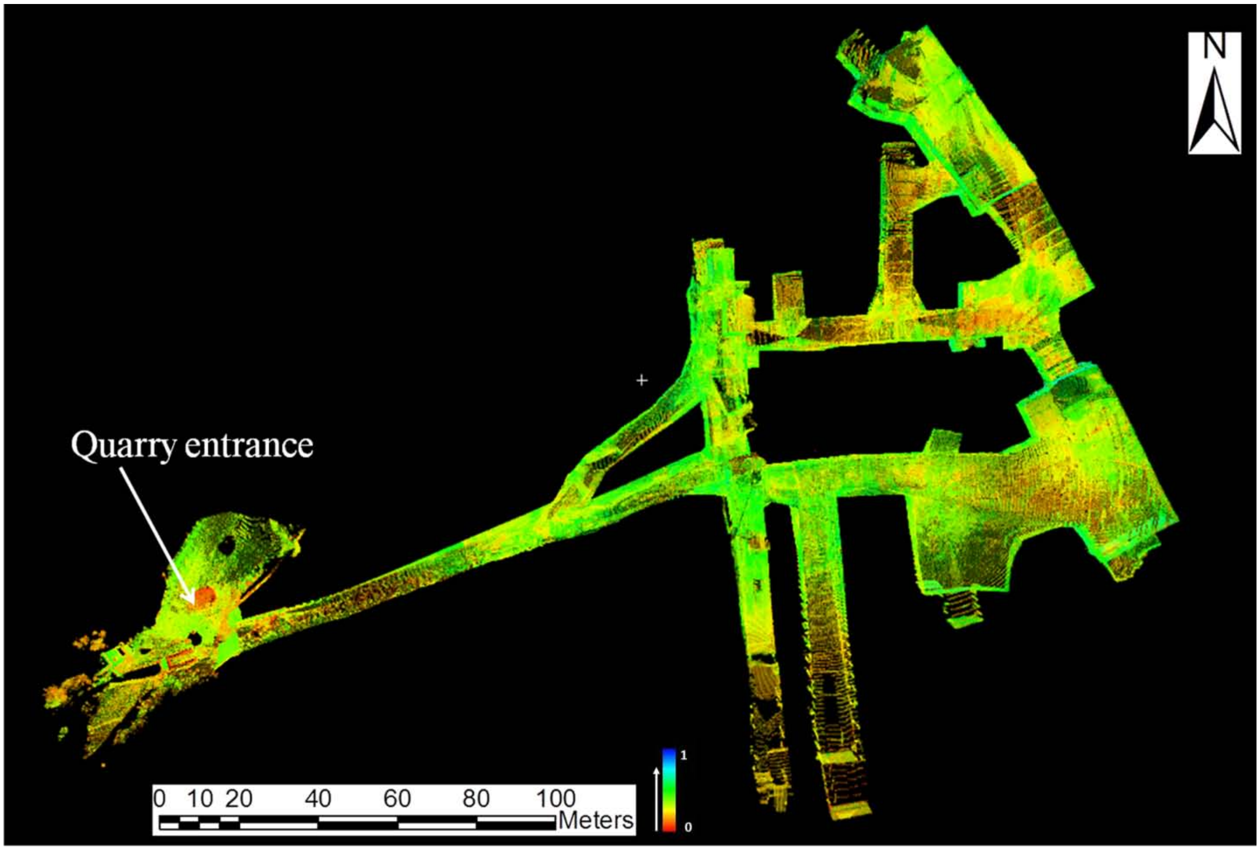

Fig. 6 – Union of all the point clouds after the registration process.

4.3 Processing of photographic data

Images were processed using *PTGui* (*New House Internet Services BV*©) and *Pano2QTVR Gui* (*Garden Gnome Software*©) which generated a 360° panorama view from every scan position (Fig. 7). The information was then mapped to the point clouds by colouring every individual point via a texturing process. Then, by using a free software routine called *Leica*™ *TruView*, a panoramic high definition point cloud viewer was created. By this viewer it is possible to extract 3D coordinates and make measurement of distances. This tool proved very useful for geological and engineering-geological surveying, both in planning the fieldwork activities and in checking the results.

Fig. 7 - Example of a panorama view created for a single scan position.

5 Output preparation and results

5.1 Topographic map creation

Starting from the final point cloud that emerges from the registration of all the scans, it was possible to create a new topographic map of the area at a scale of 1:500. The huge number of points from TLS made it possible to extract all the information sought with high accuracy and short working times. Using *Leica*^{TM} *Cyclone 8.0* it was possible to create linear features representing rooms, pillars, quarry buildings, paths, waste, and all other elements needed in a detailed topography of an underground quarry. Spot heights were extracted from specific points chosen within the point cloud. Subsequently, all the data were edited in a CAD environment and integrated with the regional technical map (*Cartografia Tecnica Regionale* - CTR) at a scale of 1:2,000. This procedure was necessary to insert the contours of the external zones of the quarry into the new topographic map (Fig.8). For better representation of the quarry, four cross sections were produced; Fig. 8 shows an example of section S1-S1'.

Based on the accuracy of the georeferenced point cloud and the comprehensive nature of the information, the resulting topographic map more than meets the intended tolerances. The updated topography, together with point clouds and high resolution photographs, is an important aid in controlling quarrying activities, guaranteeing safety in the working spaces, and producing additional deliverables. The realization and validation of the new topographic map was successfully used to create a new geological map and relative cross sections, from which a three-dimensional geological model was produced.

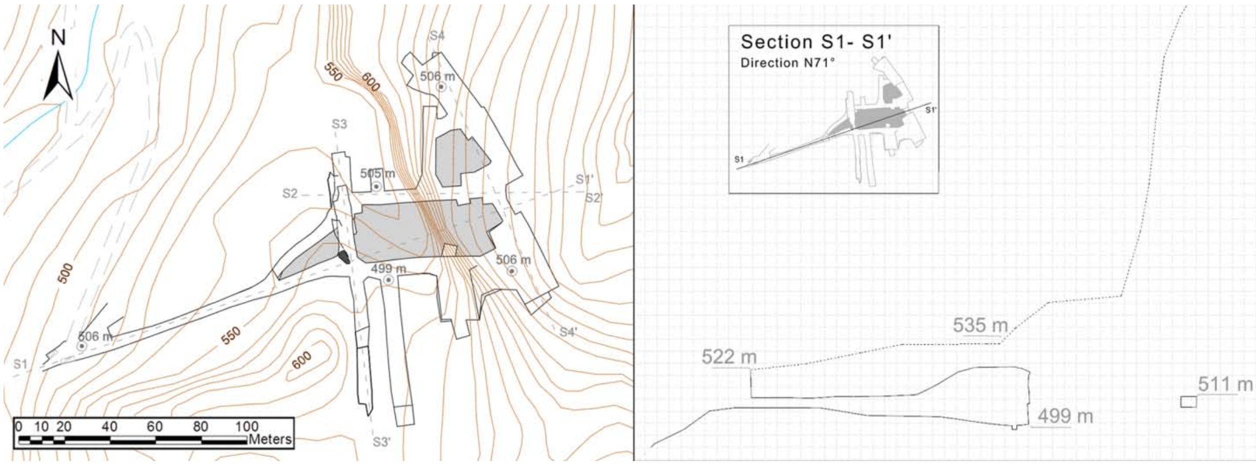

Fig. 8 – Sketch of the new topographic map (left) and example of cross section S1-S1' (right).

5.2 Underground quarry 3D modelling

A procedure, similar to the one described for extracting the linear features from the point cloud in the realization of the topographic map, was used to represent the 3D model of the quarry area. On the point clouds, the edges of natural surfaces of morphological relevance, and the anthropogenic surfaces related to the excavation activity, were demarcated. Lines were elaborated by means of *Rhinoceros*^{TM} software in order to obtain *Non Uniform Rational Basis-Spline* surfaces (NURBS) that correspond most accurately to the geometry of the excavation area (Fig. 9). The result of this operation, shown in Fig. 10, is the georeferenced three dimensional model of the entire quarry.

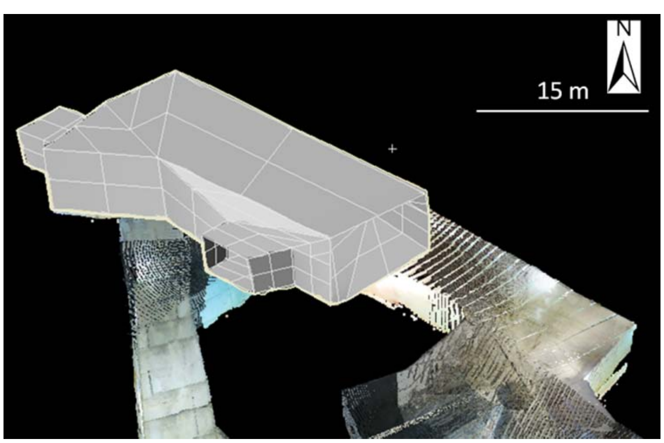

Fig. 9 – Perspective view of part of the underground quarry. NURBS surfaces are shown in grey (the scale bar is indicative only).

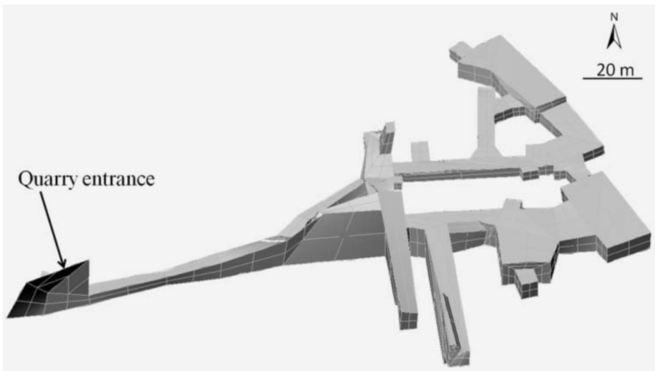

Fig. 10 – Perspective view of the 3D model of the entire underground quarry (the scale bar is indicative only).

The choice of an approach that does not involve the creation of a complex MESH from the point cloud, in favour of NURBS generation, was because of the huge quantity of data, which makes processing difficult even for powerful computers because of the large requirement for memory and high-end video cards. For this reason the point clouds, if processed by meshing, should undergo a significant reduction, which involves an undesirable loss of information and accuracy. Even the manual drawing by NURBS involved a loss of detail, but there were also important advantages such as a greater control, good celerity and easier management of the operations. Furthermore the accuracy of the final 3D model was considered still acceptable.

Moreover, these operations turned out to be much easier to manage using NURBS surfaces than MESH, as will be afterwards explained. The model was realized without need to represent those elements useless for the purpose of this work. The operator's expertise and skill were consequently needed when representing to good accuracy and completeness the relation between the quarry shape and the geological structure.

5.3 Geological 3D modelling

The 3D geological model was constructed based on the geological map and the related cross sections. The volumes of distinct formations were arbitrarily delimited: the upper boundary was represented by the Digital Terrain Model (DTM) originating from CTR, and the lower and the lateral ones by horizontal and vertical planes. The base of the model was placed at 550 meters below the quarry entrance, and the lateral boundaries at 600 and 300 meters from the same access (Fig. 11). Even the geological model was elaborated by *Rhinoceros*^{TM} *by* means of NURBS surfaces interpolated between the arcs of the geological map and cross sections that represent the above- and underground contacts. Wherever possible, only the arcs representing certain portions of geological contacts (directly observed during the geological survey) were used. The inferred contacts, which are uncertain because they are hidden or located in inaccessible areas, were used in reconstructing the model surfaces only if necessary. Aiming of simplifying the 3D model the Cherty Limestones Formation was not included. This is justified by the fact that in the area underlying the quarry (geological cross section number 2 and 3 of Fig. 3) such formation is present at a altitude lower than 300 m and does not interest in any way the exploitable area.

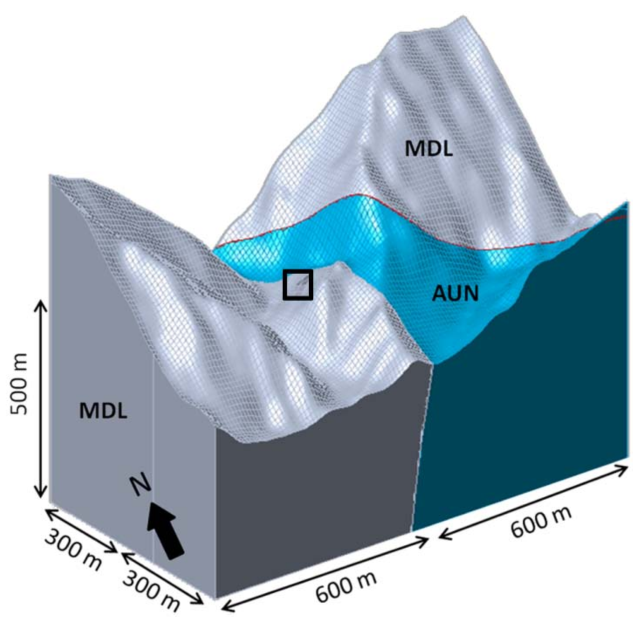

Fig. 11 – Perspective view of the 3D geological model (the quarry entrance is highlighted with a black rectangle); AUN=Marble Formation, MDL=Dolomitic Marble Formation.

5.4 Integration of 3D models

To determine the location of exploitable rock from the present shape of the quarry and the marble structure and outcrops, an integration of the two 3D models (underground quarry and geology) was undertaken. This final 3D model was used to assess the accuracy of the geological map and the relative cross sections: if the geological map and cross sections were correct, then the 3D quarry model should intersect the geological model consistently with the field observations made during the underground surveying. In this step it should be underlined the importance of the availability of detailed TLS data and high resolution images that allowed for the examination of the quarry rapidly and directly in laboratory. In addition, the georeferenced point cloud and the *Leica^{TM} TruView* viewer make it possible to draw lines in correspondence with geological contacts, faults, and any other elements of interest. These lines can then be imported into the final model. If any incongruities were detected (for example if a geological contact did not cross the quarry in the exact position) then the geological sections were modified, and eventually also the geological map.

After correction of the model, final vertical and horizontal sections were realized, facilitating analysis of the actual shape of the quarry in relation to the marble structure and outcrops (Figs. 12 and 13).

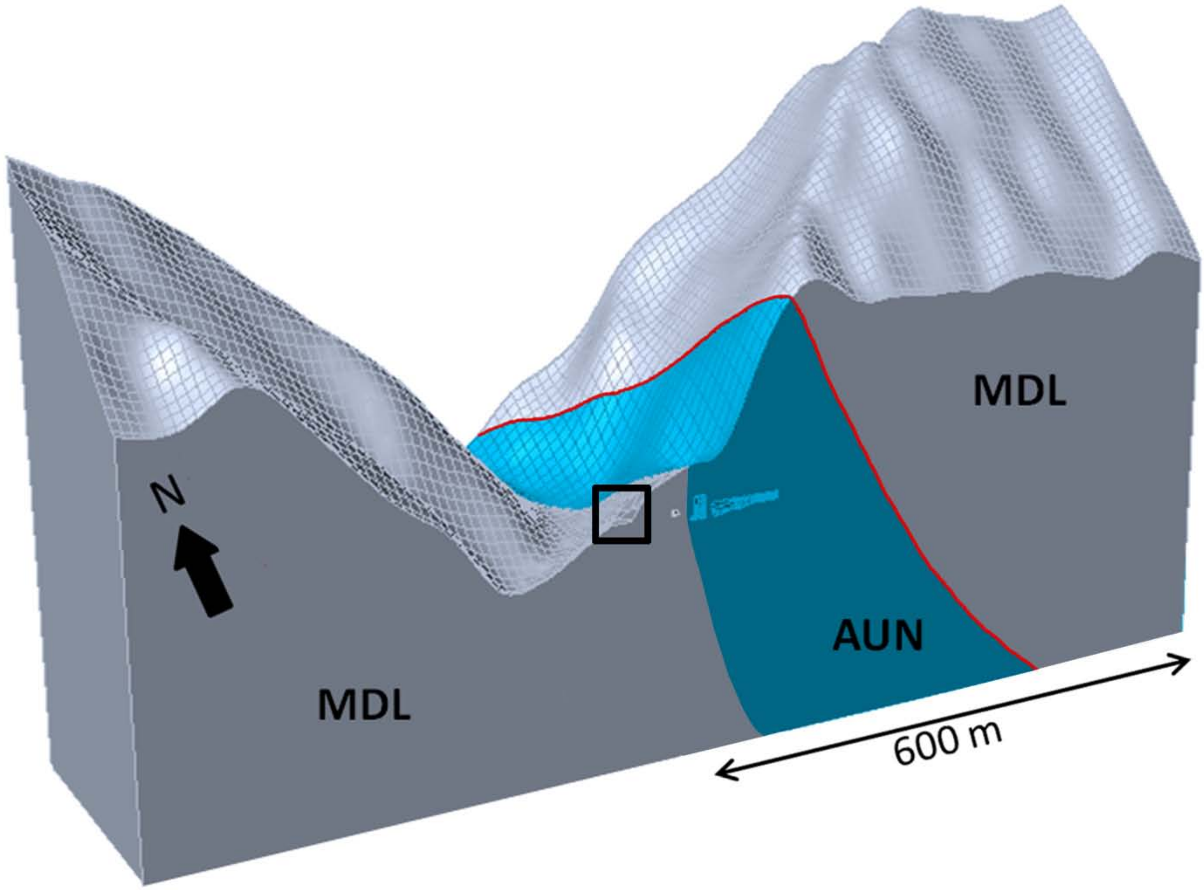

Fig. 12 – Perspective view of the 3D model corresponding to the geological cross section n°3 (the model shows the quarry entrance highlighted with a black rectangle); AUN=Marble Formation, MDL=Dolomitic Marble Formation; within the Marble Formation it is possible to note the quarry’s layout in light blue colours.

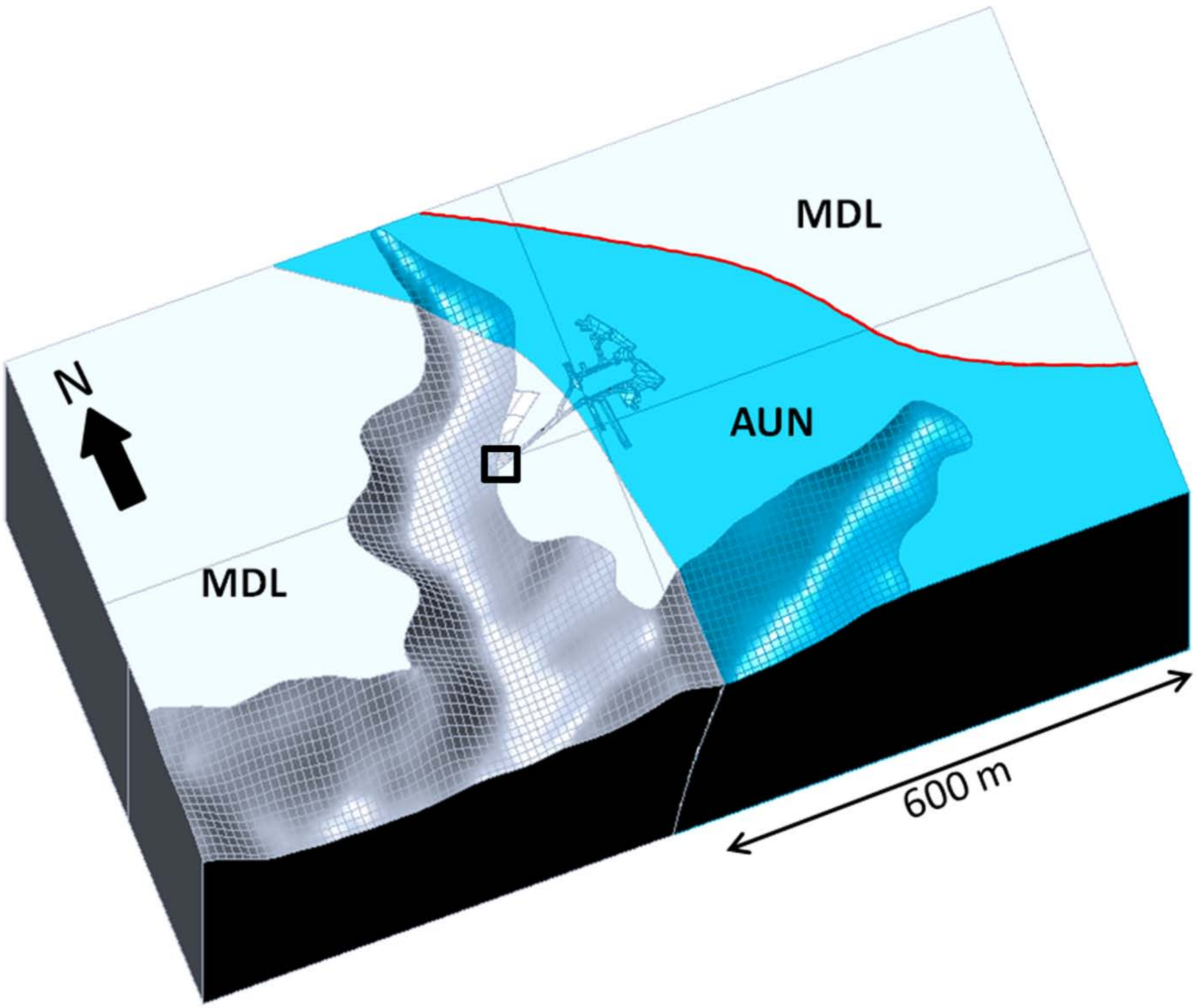

Fig.13 – Perspective view of a 3D horizontal section positioned at 515 m a.s.l. (the model shows the quarry shape with the entrance highlighted with a black rectangle); AUN=Marble Formation, MDL=Dolomitic Marble Formation.

Such a model will allow to make measurements of distance and volume, facilitating undoubtedly cultivation plans redaction. According to the final 3D model for example, further marble exploitation, as shown in Fig. 13, is possible by proceeding eastward about one hundred meters. Any updating of the TLS following further marble extraction will involve only short working times allowing multi-temporal comparisons.

5.5 Characterization of discontinuities

A structural and engineering-geological survey of the rock discontinuities was also carried out, with the aim of exploiting the knowledge gained about the stability of the walls and the safety conditions of the quarry. The *Leica™ TruView* viewer proved to be an important tool in this activity. Thanks to the high resolution of the photographic images it was possible to recognize and collect 3D coordinates of points corresponding to several discontinuities, faults and joints on screen (Fig. 14).

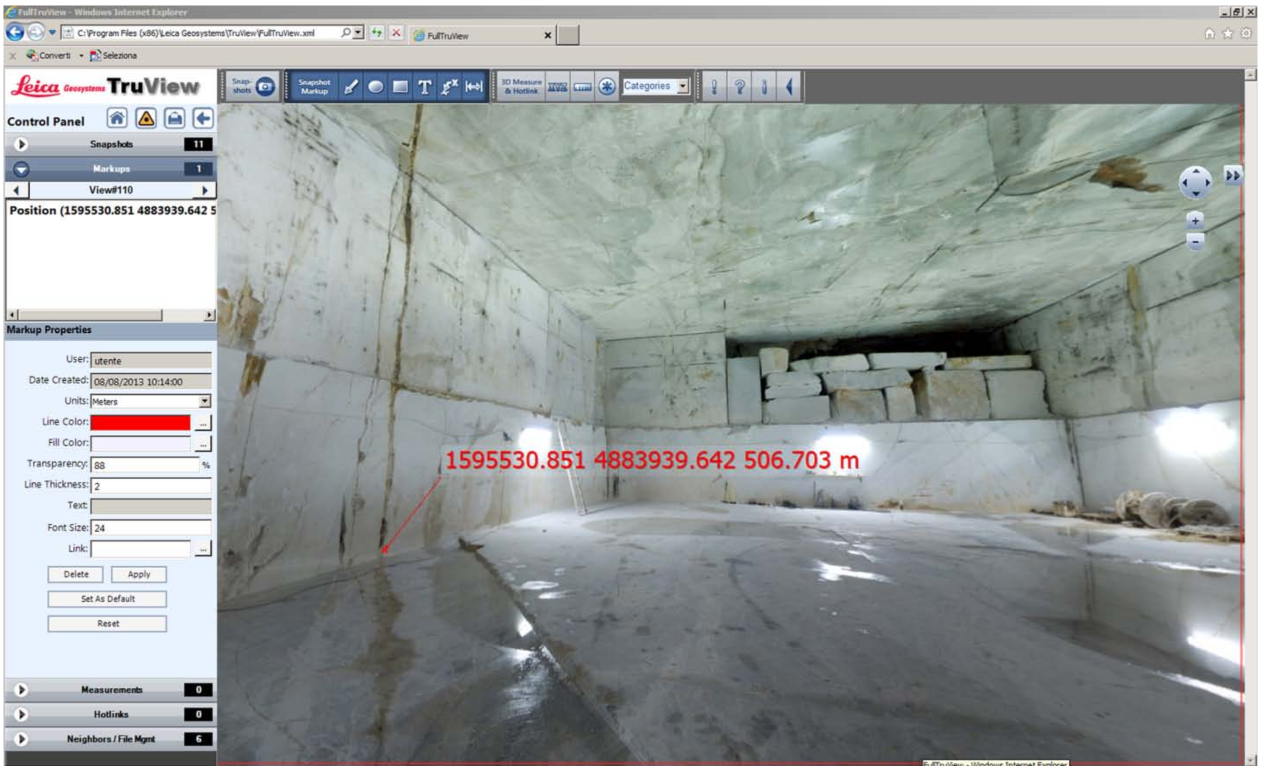

Fig. 14 - Example of Leica ™ Truview viewer with 3D coordinates referred to the position of a single point belonging to a normal fault.

This viewer was very helpful both in an earlier stage of the survey planning and during the survey itself, because it overcame the problem of the unavailability of GPS signal underground. With this method it was possible to measure the coordinates of three or more points coplanar with a discontinuity in different walls of the quarry, and then compute the dip and the dip direction of the plane containing them. The attitudes of various joints and faults were then determined in laboratory, and subsequently verified during the engineering-geological survey. Moreover, *Leica™ TruView* permitted to export and import **.xml* files that were compiled by assigning IDs and attributes to the joints. Some of these attributes (dip and dip direction, spacing, persistence and length) were compiled in laboratory and verified during the engineering-geological survey; the rest of the structural and engineering-geological info were measured during fieldwork (aperture, weathering, filling, roughness, water condition, joint wall compressive strength - JCS - Deere and Miller, 1966 and joint roughness coefficient – JRC - Barton, 1973). No kinematic indicators were recognized inside the tunnels due to the unfavourable exposition of discontinuity outcrops and to the quarrying activity that gives a regular cubic shape to the walls.

The availability of *Leica*^{TM} *TruView* files made it possible to use a notebook during fieldwork and to fill in the table of attributes related to the engineering-geological survey directly in a digital format.

Three main sub-vertical systems of discontinuities were recognized, K1 (subdivided into K1a-K1b because of its variable westward or eastward dip), K2 (subdivided into K2a-K2b because of its variable south-westward or north-eastward dip), and K3 (subdivided into K3a-K3b because of its variable south-eastward or north-westward dip). Fig. 15 shows the contour plots of the identified joint systems and the modal values of the surveyed engineering-geological parameters.

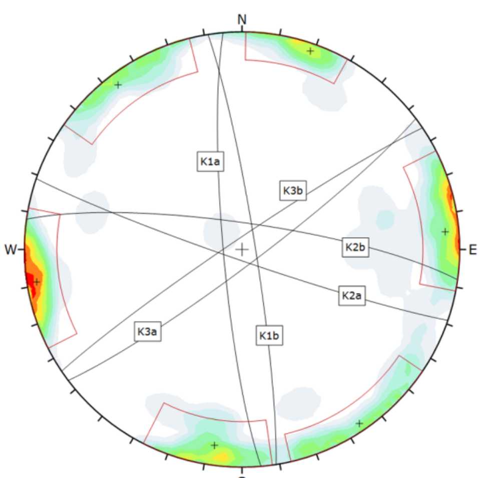

System	Dip	Dip Direction
Mean Set Planes		
K1a	83	265
K1b	85	81
K2a	86	199
K2b	80	8
K3a	84	143
K3b	86	326

System	Parameters	Description
K1	Persistence	>20 m
	Spacing	1 m
	Aperture	1-5 mm
	Roughness	slightly rough
	Filling	soft <2 mm
	Weathering	Slight
	Water condition	Dripping
K2	Persistence	>20 m
	Spacing	0,2 m
	Aperture	>5 mm
	Roughness	slightly rough
	Filling	Soft >2 mm
	Weathering	Slight
	Water condition	Wet
K3	Persistence	>20 m
	Spacing	0,5 m
	Aperture	>5 mm
	Roughness	Smooth
	Filling	Soft >2 mm
	Weathering	Slight
	Water condition	Wet

Fig. 15 - Contour plots and characteristics of joint systems from engineering-geological survey. Data is presented using stereographic projection through the Schmidt equal-area method.

As well as the three main identified systems, the main foliation (Sp), modified during the D2 phase, is present in many walls of the quarry. Its attitude testifies the presence of the Monte Rasori antiform and represents a plane of weakness that changes its dipping along the quarry, from sub-vertical to about 50°. Fig. 16 shows the map of the main measured discontinuities and the foliation.

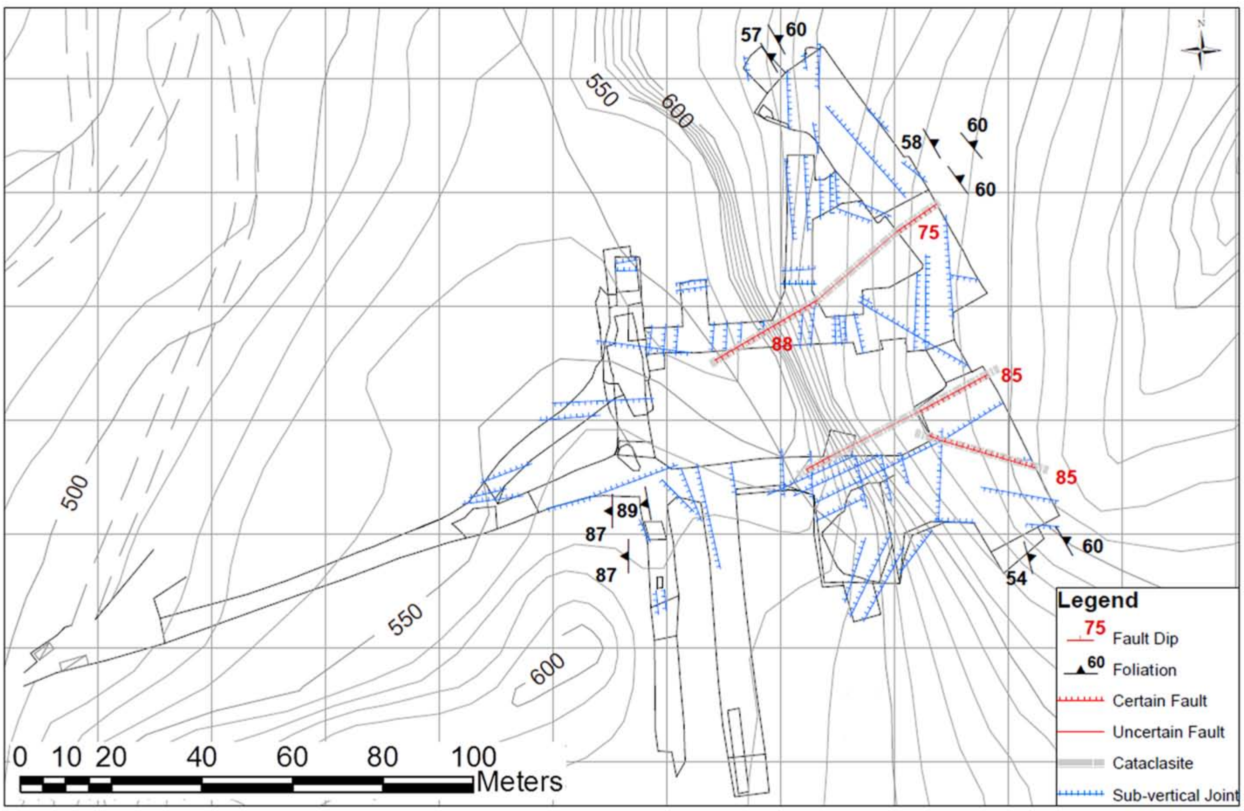

Fig. 16 - Map of the main measured discontinuities and foliation.

With the aim of contextualizing the brittle systems observed inside the underground quarry, a further discontinuity survey was carried out in the surrounding area. Directly from outcrops analysis by using conventional structural techniques and interpretation of aerial photographs and DTM from aerial LIDAR (made available by Tuscany Region), three principal discontinuity systems were measured in the Marble and Dolomitic Marble Formations.

The principal system is characterized by a general N-S orientation (Fig. 17), sub-vertical dip, hundreds of meters persistence almost parallel to the bedding plane, metric spacing, and absent filling. On this system two generations of kinematic indicators (slickensides type) with different dipping were identified: toward North and South with a pitch ranging from 25° to 45°. The lack of evidences has precluded the direct estimates of the sense of displacement and the formulation of any hypotheses about the chronological order of the indicators.

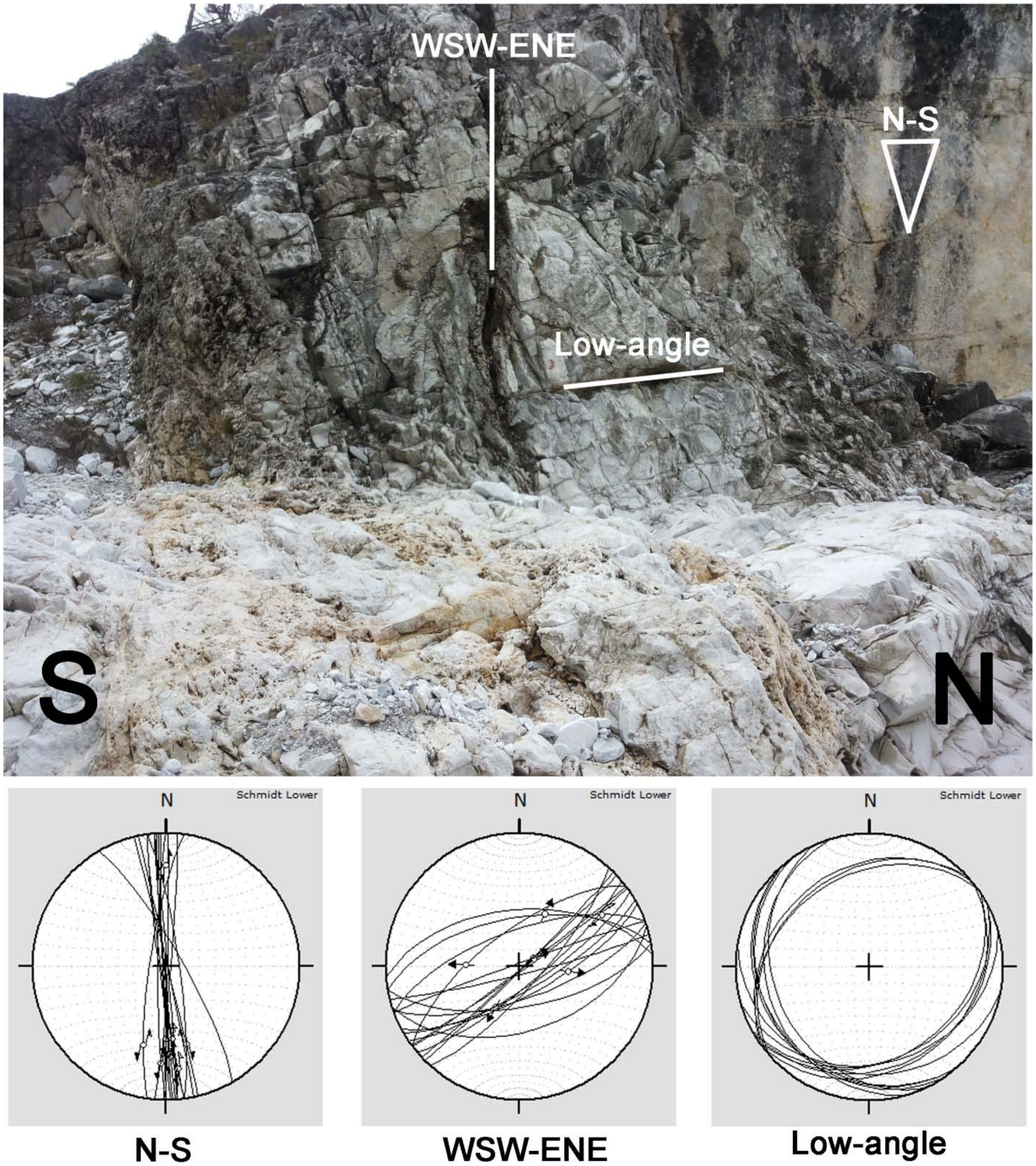

Fig. 17 – Outcrop of discontinuity systems measured out of the underground quarry (top); stereographic projections of discontinuities through the Schmidt equal-area method (bottom).

The second system is characterized by a general WSW-ENE orientation, sub-vertical dip, hundreds of meters persistence, and metric spacing. Locally in these discontinuities the presence of cataclasite with variable thickness ranging from centimetric to decimetric was identified. The cataclasite is composed by fragments of marble or dolomitic marble with size variable from millimetric to centimetric, surrounded by a finer grained matrix. The matrix is composed by calcite and sometimes it is enriched in oxides and clay minerals. Kinematic indicators (mineral growth, ploughing and slickensides) were observed on these surfaces. In this case, the indicators have allowed to clearly identify a sense of displacement typical of direct faulting (Fig. 18A).

From the above descriptions, it is possible to associate the K2 and K3 sets measured in the underground quarry to the N-S and WSW-ENE oriented systems. Moreover, in the two faults of the K3 system that are shown in Fig. 16, an apparent motion of about 1 meter was observed (example in Fig. 18B); considering also the kinematic indicators observed on similar discontinuities in the surrounding area of the quarry, it is connectable to a direct fault activity.

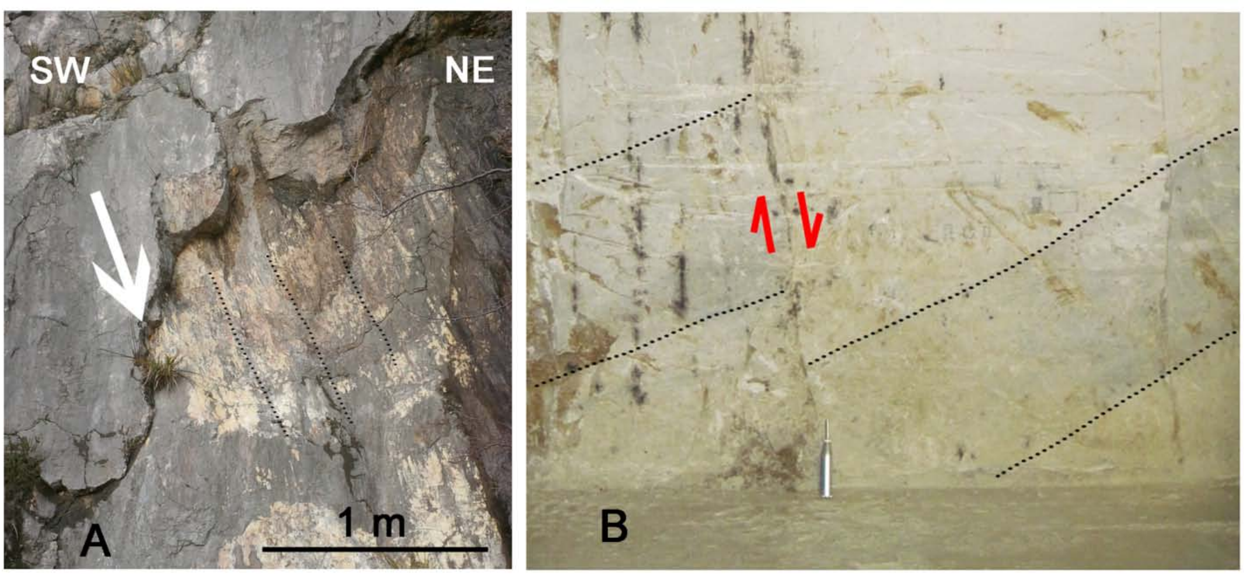

Fig. 18 – Examples of fault structures observed outside (A) and inside the quarry (B).

In addition to these systems, a third set of discontinuities, characterized by low-angle dip, metric spacing and absent filling, was recognized (this system is not present inside the quarry).

The interpretation of aerial photographs and DTM permitted to highlight the importance of the described joint systems since they influence the hydrographic pattern with an angular shape parallel to the discontinuity orientation.

Studies on brittle systems were carried out in the Carrara area by Ottria and Molli (2000). They suggested tentatively that the developed brittle structures, formed during a protracted history of deformation in which an initially mutually interfering system of strike-slip and normal faulting was followed by the development of normal faults (Molli et al., 2010), can be related to a late stage of the D2 phase and bracketed between the late Pliocene and the middle Pleistocene. Despite systematic studies about brittle structure development of the entire Apuan massif have still to be conducted, the evidences in the Romana area allow to relate the observed joint sets to the same D2 phase.

Further developments of the present work will conduct toward the stability analysis of the quarry walls: the detected orientation, persistence, and spacing of the discontinuity systems can isolate volumes of rock that can lead to instability of the fronts, influencing the excavation activity. However that may be, the authors want to underline that this paper does not detail the characterization of the rock mass or the stability analysis, but has shown how geomatics can be used in several ways in tackling geological problems in underground quarries. Fig. 19 sets out a flowchart that summarizes all the procedures involved; it allows for a new geological interpretation if the final model is clearly inconsistent with the geological map.

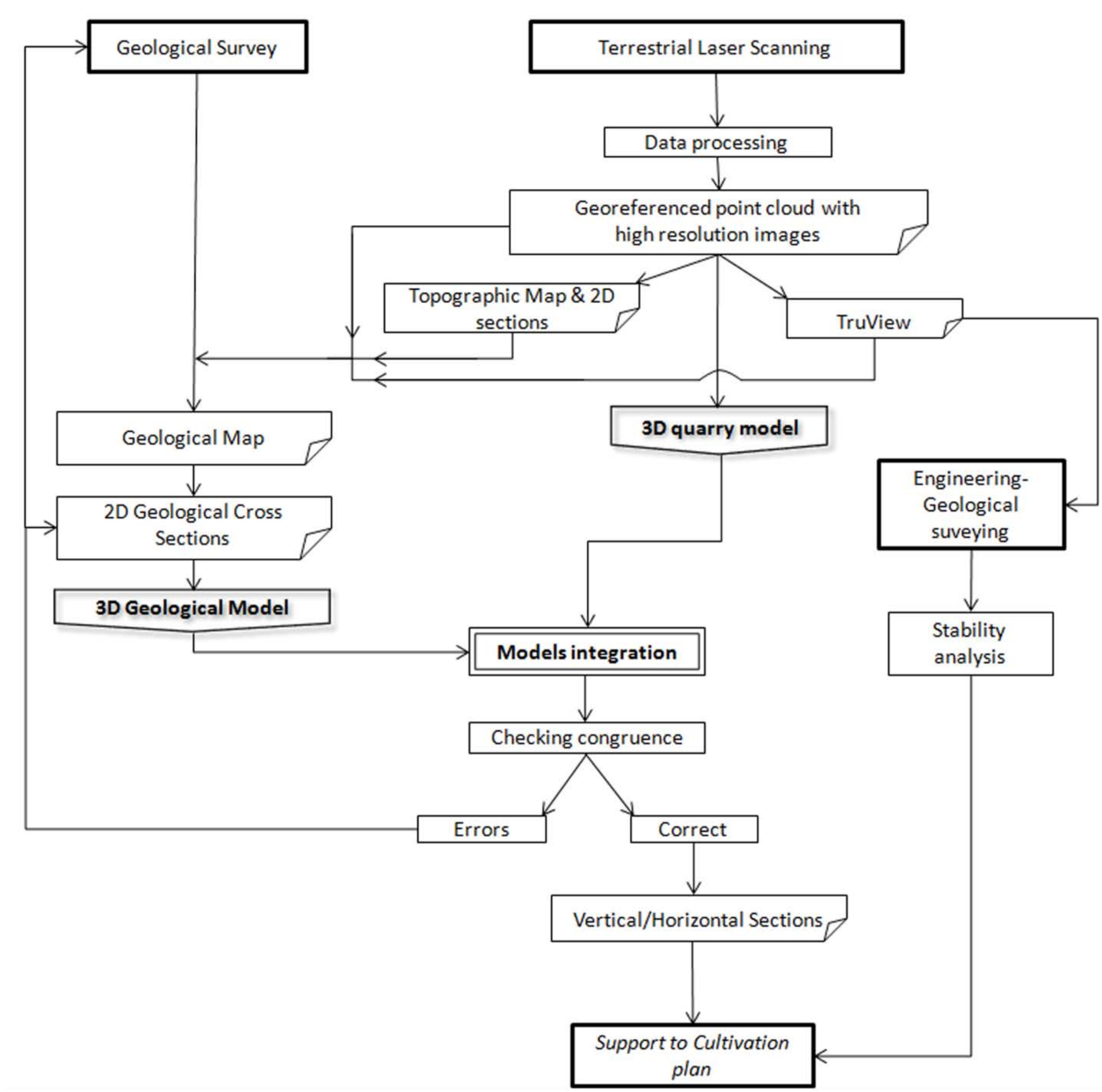

Fig. 19 - Workflow of the illustrated working approach.

6 Conclusions

This paper has presented a working approach for integrating modern techniques such as Terrestrial laser scanning with traditional ground geological surveying, with the aim of realizing a three-dimensional geological model of an underground marble quarry located in the Apuan Alps (Italy).

The rapidity, accuracy, and detail of data involved in this approach make it a powerful tool for three-dimensional characterization of underground quarrying activities, for which classical surveying techniques require longer working times and are less accurate.

The methodology was applied successfully and led to the realization of a complete three-dimensional model of the study area, from which the relations between the quarry and marble geological structure were made clear. This information, together with the engineering-geological data, is fundamental in the preparation of suitable cultivation plans. The quantity and the quality of the data obtained facilitate improvement of workplace security and allow reliable evaluation of productivity.

The advantages of this approach can be summarized as follows:

- Capability of obtaining very large amounts of geometric data (millions of points) and high resolution photographic images in short working times, due to the rapidity of TLS.
- High quality of the measured data, with centimetric accuracy.
- Simple management of the 3D topographic and geological models due to the use of NURBS surfaces rather than MESH (powerful computers are not necessary).
- High quality photographic data and 3D models that allow direct checking of correctness of the geological map and cross sections.
- Ready understanding of the relations between quarry activities and marble structure.
- Accurate measurements of volumes and distances.
- Support for engineering-geological surveys necessary for stability analysis of walls and slopes.

Acknowledgments

The authors gratefully acknowledge the assistance of the personnel of the Romana Quarry and particularly Geol. Massimo Corniani. This paper was possible because of support from the Tuscany Region Research Project known as “Health and safety in the quarries of ornamental stones - SECURCAVE".

6. References

Abellán, A., Jaboyedoff, M., Oppikofer, T., Vilaplana, J.M., 2009. Detection of millimetric deformation using a terrestrial laser scanner: experiment and application to a rockfall event. Natural Hazards and Earth System Sciences, 9, 365-372.

Armesto, J., Ordonez, C., Alejano, L., Arias, P., 2009. Terrestrial laser scanning used to determine the geometry of a granite boulder for stability analysis purposes. Geomorphology, 106, 271-277.

Barton, N.R., 1973. Review of a new shear strength criterion for rock joints. Engineering Geology, 7, 287-332.

Bertacchini, E., Boni, E., Capitani, A., Capra, A., Castagnetti, C., Corsini, A., Dubbini, M., Parmeggiani, E., 2009. Stazione totale per il monitoraggio Leica TM30: test di verifica secondo norme DIN-18723 e test di funzionamento per il monitoraggio frane. In: Atti Asita 2009, Bari, Italy, pp. 373-374. ISBN 978-88-903132-2-6.

Beshr, A.A.A., Elnaga, I.M.A., 2011. Investigating the accuracy of digital levels and reflectorless total stations for purposes of geodetic engineering. Alexandria Engineering Journal, 50, 399-405, ISSN 1110-0168, http://dx.doi.org/10.1016/j.aej.2011.12.004.

Boehler, W., Bordas Vicent, M., Marbs, A., 2003. Investigating Laser Scanner Accuracy. In: Proceedings of the XIXth CIPA Symposium. ISPRS/CIPA, Antalya, Turkey, pp. 696-701.

Carmignani, L., Kligfield, R., 1990. Crustal extension in the Northern Apennines: the transition from compression to extension in the Alpi Apuane core complex. Tectonics, 9, 1275-1303.

Carmignani, L., Conti, P., Fantozzi, P., Mancini, S., Massa, G., Molli, G., Vaselli, L., 2007. I marmi delle Alpi Apuane, In: Geoitalia, 21,19-30.

Carmignani, L., Disperati, L., Fantozzi, P.L., Giglia, G., Meccheri, M., 1993a. Tettonica distensiva del Complesso metamorfico Apuano. Guida all’escursione. Gruppo informale di Geologia Strutturale, Siena, 128 pp.

Carmignani, L, Fantozzi, P.L., Giglia, G., Meccheri, M., 1993b. Pieghe associate alla distensione duttile del complesso metamorfico apuano. Memorie Società Geologica Italiana, 49, 99-124.

Carmignani, L., Giglia, G., Kligfield, R., 1978. Structural evolution of the Apuane Alps; an example of continental margin deformation in the northern Apennines, Italy. Journal of Geology, 86, 487-504.

Conti, P., Carmigani, L., Giglia, G., Meccheri, M., Fantozzi, P. L., 2004. Evolution of geological interpretations in the Alpi Apuane Metamorphic Complex, and their relevance for the geology of the Northern Apennines. In: The “Regione Toscana” project of geological mapping (Geological Survey of Tuscan Region, Florence), pp. 241-262.

Deere, D.U., Miller, R.P., 1966. Engineering classification and index properties for intact rock. Technical Report AFNL-TR-65-116. Air Force Weapons Laboratory, New Mexico, 277 pp.

Elter, P., 1975. Introduction à la géologie de l'Apennin septentrional. Bulletin de la Societe Geologique de France 7, 956-962.

Fekete, S., Diederichs, M., Lato, M., 2010. Geotechnical and operational applications for 3-dimensional laser scanning in drill and blast tunnels. Tunnelling and Underground Space Technology, 25, 614-628, ISSN 0886-7798, 10.1016/j.tust.2010.04.008.

Fellin, M.G., Reiners, P.W., Brandon, M.T., Wuthrich, E., Balestrieri, M.L., Molli, G., 2007. Thermochronologic evidence of exhumational history of the Alpi Apuane metamorphic core complex, northern appennines, Italy. Tectonics, 26, TC6015, doi:10.1029/2006TC002085.

Ganić, A., Milutinović, A., Tokalić, R., Ognjanović, S., 2011. Measuring methods for cross sections of underground mine chambers. Underground mining engineering 19, 101-108.

Hill, C.D., Sippel, K.D., 2002. Modern Deformation Monitoring: A Multi Sensor Approach. In: Proc. XXII FIG International Congress, International Federation of Surveyors, Washington, D.C..

Kirschner, H., Stempfhuber, W., 2008. The kinematic potential of modern tracking total stations a state of the art report on the Leica TPS1200+. In: 1st international conference on machine control & guidance 2008, Zurich.

Kligfield, R., Hunziker, J., Dallmeyer, R.D., Schamel, S., 1986. Dating of deformational phases using K-Ar and ^{40}Ar/^{39}Ar techniques:results from the Northern Appennines. Journal of Structural Geology, 8, 781-798, doi:10.1016/0191-8141(86)90025-8.

Kontogianni, V., Kornarou, S., Stiros, S., 2007. Monitoring with electronic total stations: Performance and accuracy of prismatic and non-prismatic reflectors. Geotechnical News, 25, 30-3.

Lato, M., Diederichs, M.S., Hutchinson, D. J., Harrap, R., 2009. Optimization of LiDAR scanning and processing for automated structural evaluation of discontinuities in rockmasses. International Journal of Rock Mechanics and Mining Sciences, 46, 194-199, ISSN 1365-1609, 10.1016/j.ijrmms.2008.04.007.

Leica SmartNet ItalPos, 2013. Satellite Positioning Services. <http://it.smartnet-eu.com/rinex-30-sec_568.htm> (Accessed: 18 February 2013)

Lemy, F., Yong, S., Schulz, T., 2006. A case study of monitoring tunnel wall displacement using laser scanning technology. In: The 10th IAEG International Congress, IAEG2006, Nottingham, United Kingdom. (Paper number 482)

Lichti, D.D., Licht, M.G., 2006. Experiences with terrestrial laser scanner modelling and accuracy assessment. In: Proceedings IAPRS, Dresden, Germany, 26, 155-160.

Lichti, D. D., Jamtsho, S., 2006. Angular Resolution of Terrestrial Laser Scanners. The Photogrammetric Record: An International Journal of Photogrammetry 21, 141-160.

Mechelke, K., Kersten, T.P., Lindstaedt, M., 2007. Comparative investigations into the accuracy behaviour of the new generation of terrestrial laser scanning systems. In A. Gruen, & H. Kahmen (Eds.), Optical 3-D Measurement Techniques, Zurich, Vol. I, pp. 319-327.

Molli, G., 2008. Northern Appennine-Corsica orogenic system: an updated review. In: S. Siegesmund, B. Fügenschuh, & N. Froidzheim (Eds.), Tectonic Aspects of the Alpine-Dinaride-Carpathian System. Geological Society of London Special Publication, 298, 413-442.

Molli, G., 2012. Deformation and fluid flow during underplating and exhumation of the Adria Continental margin: A one-day field trip in the Alpi Apuane (northern Apennines, Italy). In: P. Vannucchi and D. Fisher (Eds.), Deformation, Fluid Flow and Mass Transfer in the Forearc of Convergent Margins: Field Guides to the Northern Apennines in Emilia and the Apuan Alps (Italy). The Geological Society of America, 28, 35-48, doi: 10.1130/2012.0028(02).

Molli, G., Meccheri, M., 2000. Geometrie di deformazione nell'alta valle di Colonnata: un esempio di deformazione polifasica e composita nelle Alpi Apuane. Bollettino della Societa Geologica Italiana 119, 379-394.

Molli, G., Vaselli, L., 2006. Structures, interference patterns and strain regime during mid-crustal deformation in the Alpi Apuane (Northern Appennines, Italy). In S. Mazzoli, & R. Buler (Eds.), Styles of Continental Contraction. Geological Society of American Special Paper 414, pp. 79-93. doi:10.1130/2006.2414(05).

Molli, G., Meccheri, M., 2012. Structural inheritance and style of reactivation at mid-crustal levels: A case study from the Alpi Apuane (Tuscany, Italy). Tectonophysics, 579, 74-87.

Molli, G., Cortecci, G., Vaselli, L., Ottria, G., Cortopassi, A., Dinelli, E., Mussi, M., Barbieri, M., 2010. Fault zone structure and fluid-rock interaction of a high angle normal fault in Carrara marble (NW Tuscany, Italy). Journal of Structural Geology 32, 1334-1348. http://dx.doi.org/10.1016/j.jsg. 2009.04.021.

Molli, G., Giorgetti, G., Meccheri, M., 2000. Structural and petrological constrains on the tectono-metamorphic evolution of the Massa Unit (Alpi Apuane, NW Tuscany, Italy). Journal of Geology, 35, 251-264.

Molli, G., Giorgetti G., Meccheri, M., 2002. Tectono-metamorphic evolution of the Alpi Apuane Metamorphic Complex: new data and constraints for geodynamic models. Bollettino Sicietà Geologica Italiana, 1, 789-800.

Ottria, G., Molli, G., 2000. Superimposed brittle structures in the late orogenic extension of the northern Apennine: results from Carrara area (Alpi Apuane, NW Tuscany). Terra Nova 12, 1-8.

Pejić, M., 2013. Design and optimisation of laser scanning for tunnels geometry inspection. Tunnelling and Underground Space Technology, 37, 199-206, ISSN 0886-7798, 10.1016/j.tust.2013.04.004.

Petrie, G., Toth, K.C., 2008. Introducing to Laser Ranging, Profiling, and Scanning. In J. Shan, & K.C. Toth (Eds.), Topographic Laser Ranging and Scanning Principles and Processing, pp. 1-27.

Rotonda, T., Marsella, M., Lizzadro, L., Ricca, A., 2007. Analysis of laser scanner data collected during a survey of faces in a rock quarry. In: C. Olalla, N. Grossmann & L. Ribeiro e Sousa (Eds.), The Second Half Century of Rock Mechanics. 11th Congress of the International Society for Rock Mechanics. Lisbon 2007. Print ISBN:978-0-415-45084-3, eBook ISBN:978-0-415-88954-4.

Rykkeld, E., Fossen H., 1992. Composite fabrics in mid-crustal gneisses: observations from the Oygarden Complex, West Northway Caledonides. J. Struct. Geol., 14, 1-9.

Salvini, R, Francioni, M., Riccucci, S., Bonciani, F., & Callegari, I., 2013. Photogrammetry and laser scanning for analyzing slope stability and rock fall runout along the Domodossola–Iselle railway, the Italian Alps. Geomorphology, 185, 110-122, ISSN 0169-555X, 10.1016/j.geomorph.2012.12.020.

Sturzenegger, M., Stead, D., 2009. Quantifying discontinuity orientation and persistence on high mountain rock slopes and large landslides using terrestrial remote sensing techniques. Natural Hazards and Earth System Sciences, 9, 267-287, doi:10.5194/nhess-9-267-2009.

Voegtle, T., Schwab, I., Landes, T., 2008. Influences of different materials on the measurement of a Terrestrial Laser Scanner (TLS). In: Proc. of the XXI Congress, The International Society for Photogrammetry and Remote Sensing. (ISPRS), Vol. XXXVII, Beijing, China, pp. 1061–1066.